

# Rapidity Dependence of Charged Hadron Production in Central Au+Au Collisions at $\sqrt{s_{NN}} = 200$ GeV with BRAHMS

D. Ouerdane<sup>a</sup> for the BRAHMS Collaboration

<sup>a</sup> Niels Bohr Institute, University of Copenhagen, Denmark

**Abstract.** We have measured the rapidity distributions  $dN/dy$  of  $\pi^\pm$ ,  $K^\pm$  and  $p$ ,  $\bar{p}$  in central Au+Au collisions at  $\sqrt{s_{NN}} = 200$  GeV. The average rapidity loss per participant nucleon is  $2.0 \pm 0.2$  units of rapidity. The strange to non-strange meson ratios  $K/\pi$  are found to track variations of the baryo-chemical potential in energy and rapidity.

In ultra-relativistic heavy ion collisions, final state hadrons are used as a probe of the different reaction stages, with a special focus on observables that may reveal the existence of an early color deconfined phase, the so-called quark gluon plasma. The bulk properties of the collision dynamics are becoming well understood at mid-rapidity ( $|y| \lesssim 0.5$ ). However, in Au+Au collisions at  $\sqrt{s_{NN}} = 200$  GeV, where the beam rapidity is  $y_b = 5.36$ , this corresponds to less than 10% of the whole rapidity range ( $2 \times y_b$ ). One of the goals of the BRAHMS experiment [1] is to explore a broader rapidity range ( $-0.1 \lesssim y \lesssim 3.5$ ). In this paper, we report on some of our latest results on identified charged particle yields from the 5% most central Au+Au collisions at  $\sqrt{s_{NN}} = 200$  GeV.

BRAHMS consists of two hadron spectrometers, a mid-rapidity arm (MRS) and a forward rapidity arm (FS), as well as a set of detectors for global event characterization [1]. Particle spectra were obtained by combining data from several spectrometer settings (magnetic field and angle), each of which covers a portion of the phase-space  $(y, p_T)$ . The data have been corrected for the limited acceptance of the spectrometers using a Monte-Carlo calculation simulating the geometry and tracking of the BRAHMS detector system. Detector efficiency, multiple scattering and in-flight decay corrections

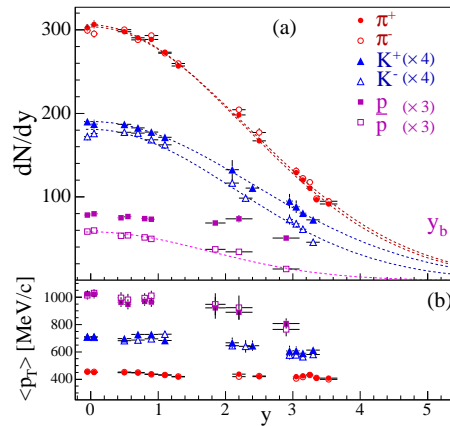


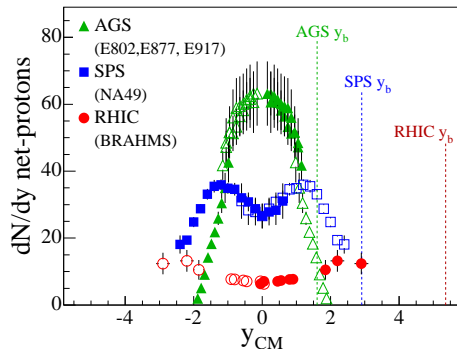
**Figure 1.**  $\pi^\pm$ ,  $K^\pm$  and  $p, \bar{p}$  rapidity distributions (a) and mean transverse momentum  $\langle p_T \rangle$  (b). Errors are statistical.

have been estimated using the same technique, but the data have not been corrected for feed-down from resonance and hyperon decays. Details can be found in [1, 2].

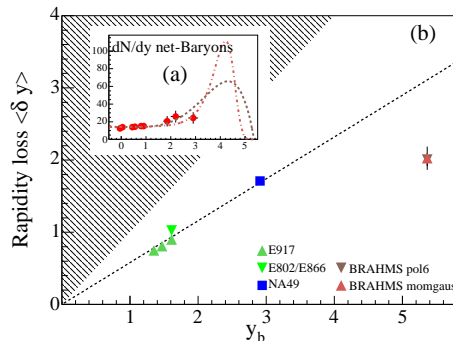
The pion and kaon spectra were well described at all rapidities by a power law in  $p_T$ ,  $A(1 + p_T/p_0)^{-n}$ , and an exponential in  $m_T - m_0$ ,  $A \exp(\frac{m_T - m_0}{T})$ , respectively. The invariant yields  $dN/dy$  were calculated by integrating the fit functions over the full  $p_T$  or  $m_T$  range. The systematic errors on  $dN/dy$ , including errors from extrapolation and normalization, amount to  $\sim 10\%$  in the range  $0 \lesssim y < 1.3$  and  $\sim 15\%$  for  $y > 1.3$ . Rapidity densities and mean transverse momenta are shown in Fig. 1. Negative and positive pions are found in nearly equal amounts within the rapidity range covered. In contrast, an excess of  $K^+$  ( $p$ ) over  $K^-$  ( $\bar{p}$ ) is observed to increase with rapidity. Figure 1(b) shows the rapidity dependence of  $\langle p_T \rangle$ . There is no significant difference between positive and negative particles of a given mass. In order to extract full phase space densities for  $\pi^\pm$  and  $K^\pm$  we have investigated several fit functions: a single Gaussian centered at  $y = 0$  (G1), a sum of two Gaussians (G2) or Woods-Saxon (WS) distributions placed symmetrically around  $y = 0$ . In Tab. 1 are reported the average yields.

**Table 1.** Full phase-space yields of  $\pi^\pm$  and  $K^\pm$  extracted from fits to the  $dN/dy$  distributions (see text). Errors reported here are statistical, systematic errors are of the order of 8%.

$\pi^+$	$\pi^-$	$K^+$	$K^-$	$\bar{p}$
$1742 \pm 17$	$1761 \pm 16$	$288 \pm 5$	$241 \pm 3$	$85 \pm 4$



**Figure 2.** Net-proton rapidity densities as a function of rapidity for three different beam energies.



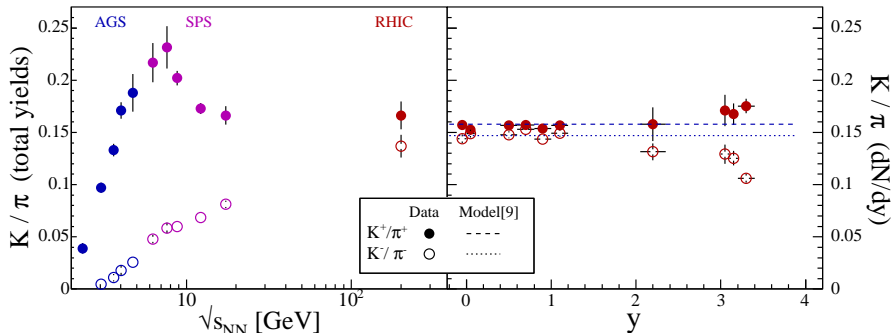
**Figure 3.** Net-baryon rapidity distributions (a) and average rapidity loss per participant nucleon as a function of beam rapidity (b). Errors are systematic.

Figure 2 shows the net-proton densities  $dN/dy(p) - dN/dy(\bar{p})$  as a function of rapidity. Our data [3, 4] (red circles) are plotted together with AGS [5, 6, 7] and top SPS [8] data. A drastic change in the shape of the distribution occurs as  $\sqrt{s_{NN}}$  increases. At RHIC, the net-proton density is  $6.4 \pm 0.4 \pm 1.0$  around mid-rapidity ( $y < 1$ ) and increases to  $12.4 \pm 0.3 \pm 3.2$  at  $y \sim 3$ . This indicates that collisions are much more transparent than at AGS and SPS. The energy available for particle production is determined from the energy loss  $\Delta E$  of the original nuclei and is related

to the degree of stopping. Due to the conservation of the baryon number during the reaction, the final state net-baryon ( $B - \bar{B}$ ) distribution contains information on  $\Delta E$ . The nuclear stopping is quantified by the rapidity loss  $\langle \delta y \rangle$ , which, for mass symmetric collisions, is defined by  $\langle \delta y \rangle = y_b - \langle y \rangle$ , where  $\langle y \rangle$  is the mean net-baryon rapidity after the collision:

$$\langle y \rangle = \int_0^{y_b} y \frac{dN_{(B-\bar{B})}(y)}{dy} dy \quad (1)$$

It is therefore necessary to know the distribution of baryons in the whole rapidity range. A Monte-Carlo simulation provided corrections factors for the non-detected neutrons, and strange baryons such as  $\Lambda$ 's and  $\Sigma$ 's. Only mid-rapidity hyperon yields are known experimentally, so we made assumptions for more forward rapidities. Details can be found in [3, 4]. Since the data do not cover the entire rapidity range, the missing information has been extrapolated from the measured data by fitting the latter with a function that is continuous and whose integral is equal to the number of participants ( $357 \pm 9$  for the 5% most central collisions after a Glauber simulation). Figure 3 shows the net-baryon distribution as a function of  $y$  (insert) and  $\langle \delta y \rangle$  as a function  $y_b$  (main panel). Two functions were used: a sum of Gaussians symmetrically positioned around mid-rapidity, and a six order polynomial (dashed lines in insert). In both cases,  $\langle \delta y \rangle$  amounts to  $2.0 \pm 0.2$ . This result is significantly lower than the expectation from the empirical scale  $\langle \delta y \rangle \propto y_b$ . The energy loss, calculated after the net-baryon fits, is found to be  $\Delta E = 72 \pm 6$  GeV per participant, i.e.  $25.7 \pm 2.1$  TeV for the corresponding centrality class.



**Figure 4.** Full phase-space  $K/\pi$  ratios as a function of  $\sqrt{s_{NN}}$  (a) and rapidity systematics at  $\sqrt{s_{NN}} = 200$  GeV (b). The dashed and dotted lines in (b) are predictions of the statistical model [9]. Errors are statistical and systematic in (a), only statistical in (b). AGS data are from [10, 11], SPS data from [12, 13, 14]. Data points at  $\sqrt{s_{NN}} = 6.3$  GeV and 7.6 GeV [12, 13] are preliminary.

In Fig. 4(a) are shown ratios of the strange to non-strange full phase-space meson yields ( $K/\pi$ ) as a function of  $\sqrt{s_{NN}}$ . The ratio  $K^+/\pi^+$  shows a fast increase from low AGS to low SPS energies ( $\sqrt{s_{NN}} = 8$  GeV), followed by a decrease with increasing SPS energy (to  $\sqrt{s_{NN}} = 17$  GeV). We find, at  $\sqrt{s_{NN}} = 200$  GeV, a value of  $0.165 \pm 0.003 \pm 0.013$ , consistent with the SPS ratio at the highest energy. In contrast,  $K^-/\pi^-$  increases monotonically but remains below  $K^+/\pi^+$ . At  $\sqrt{s_{NN}} = 200$  GeV, it reaches a value of  $0.136 \pm 0.002 \pm 0.011$ , which is close to  $K^+/\pi^+$  at the same energy.

The full phase-space ratios are not significantly different from those observed in the mid-rapidity region  $y \lesssim 1$  (Fig. 4(b)). Indeed, a fit to a straight line in this particular range gives  $K^+/\pi^+ = 0.156 \pm 0.023$  (stat + syst) and  $K^-/\pi^- = 0.146 \pm 0.016$ . The dashed and dotted lines are predictions of the hadron gas statistical model [9], which used a chemical freeze-out temperature  $T$  of 177 MeV and baryo-chemical potential  $\mu_B$  of 29 MeV (the authors restricted their fits to yields measured in the rapidity range  $|y| < 0.5$ ). The agreement with the data is excellent. However, the data deviate from the model prediction at higher rapidities, where an increasing excess of  $K^+$  over  $K^-$  is observed. This is due to an increase of net-baryon densities [3, 15]. A baryon rich environment is favorable for associated strangeness production, e.g.  $p+p \rightarrow p+K^++\Lambda$ , a production channel forbidden to  $K^-$ . In the context of the statistical model, this translates into an increase of the baryo-chemical potential  $\mu_B$ , as already reported in [15], where a calculation by Becattini *et al.* [16] of  $K^+/K^-$  vs  $\bar{p}/p$  at constant  $T$  (and varying  $\mu_B$ ) agrees well with the rapidity dependence of the experimental ratios. It is also known that the chemical freeze-out temperature varies strongly in the AGS energy range but slightly from SPS to RHIC energies. In this particular energy domain, the  $K/\pi$  systematics are as well mainly driven by changes in  $\mu_B$ .

In summary, we have measured transverse momentum spectra and inclusive invariant yields of charged hadrons  $\pi^\pm$ ,  $K^\pm$  and  $p, \bar{p}$ . The net-proton densities are the lowest ever observed in heavy-ion collisions and increase only slightly with increasing rapidity. The rapidity loss calculated from the net-baryons is found to be  $\langle \delta y \rangle = 2.0 \pm 0.2$ , thus breaking the empirical scaling observed at lower energies. The ratio of strange to non strange mesons  $K/\pi$  ratios are well reproduced by the hadron gas statistical model [9] that assumes strangeness equilibration. The increasing difference between  $K^+$  and  $K^-$  yields at higher rapidities is explained by a change of the baryo-chemical potential  $\mu_B$  with increasing rapidity.

This work was supported by the division of Nuclear Physics of the Office of Science of the U.S. DOE, the Danish Natural Science Research Council, the Research Council of Norway, the Polish State Com. for Scientific Research and the Romanian Ministry of Research.

## References

- [1] M. Adamczyk *et al.* *Nucl. Instrum. Meth.*, A499:437–468, 2003.
- [2] D. Ouerdane. PhD thesis, Copenhagen University, 2003.
- [3] I. G. Bearden *et al.* *nucl-ex/0312023*, 2003.
- [4] P. H. L. Christiansen. PhD thesis, Copenhagen University, 2003.
- [5] B. B. Back *et al.* *Phys. Rev. Lett.*, 86:1970, 2001.
- [6] L. Ahle *et al.* *Phys. Rev.*, C60:064901, 1999.
- [7] L. Barette *et al.* *Phys. Rev.*, C62:024901, 2000.
- [8] H. Appelshauser. *Phys. Rev. Lett.*, 82:2471, 1999.
- [9] P. Braun-Munzinger, D. Magestro, K. Redlich, and J. Stachel. *Phys. Lett.*, B518:41–46, 2001.
- [10] L. Ahle *et al.* *Phys. Rev.*, C57:466–470, 1998.
- [11] L. Ahle *et al.* *Phys. Lett.*, B476:1–8, 2000.
- [12] C. Alt *et al.* *J. Phys.*, G30:S119–S128, private communication, 2004.
- [13] M. Gaździcki *et al.* In *Proceedings of Quark Matter 2004*, 2004.
- [14] S. V. Afanasiev *et al.* *Phys. Rev.*, C66:054902, 2002.
- [15] I. G. Bearden *et al.* *Phys. Rev. Lett.*, 90:102301, 2003.
- [16] F. Becattini, J. Cleymans, A. Keranen, E. Suhonen, and K. Redlich. *Phys. Rev.*, C64:024901, 2001.